TITLE

Arctic Ocean's wintertime Mercury concentrations limited by seasonal loss on the shelf

AUTHOR LIST

Stephen G. Kohler*[1]

Lars-Eric Heimbürger-Boavida*[2]

Mariia V. Petrova[2]

Maria G. Digernes[1]

Nicolas Sanchez[1]

Aurélie Dufour[2]

Anica Simić[1]

Kuria Ndungu[3]

Murat V. Ardelan*[1]

AFFILIATIONS

[1]Norwegian University of Science and Technology (NTNU), Department of Chemistry, Trondheim, Norway

[2]Aix Marseille Université, CNRS/INSU, Université de Toulon, IRD, Mediterranean Institute of Oceanography (MIO), Marseille, France

[3]Norwegian Institute for Water Research (NIVA), Oslo, Norway

---

ABSTRACT

High biota mercury levels are persisting in the Arctic, threatening ecosystem and human health. The Arctic Ocean receives large pulsed mercury inputs from rivers and the atmosphere. Yet, the fate of those inputs and possible seasonal variability of mercury in the Arctic Ocean remain uncertain. Until now, seawater observations were only possible during summer and fall. Here we report polar night mercury seawater observations on a gradient from the shelf into the Arctic Ocean. We observed lower and less variable total mercury concentrations during the polar night (0.46 ± 0.07 pmol L^{-1}) compared to summer (0.63 ± 0.19 pmol L^{-1}) and no significant changes in methylmercury concentrations (summer, 0.11 ± 0.03 pmol L^{-1} and winter, 0.12 ± 0.04 pmol L^{-1}). Seasonal changes were estimated by calculating the difference in the integrated mercury pools. We estimate losses of inorganic mercury of 208 ± 41 pmol m^{-2} d^{-1} on the shelf driven by seasonal particle scavenging. Persistent methylmercury concentrations (-1 ± 16 pmol m^{-2} d^{-1}) are likely driven by gaseous species and a lower affinity for particles. Our results update the current understanding of Arctic mercury cycling and require budgets and models to be reevaluated with a seasonal aspect.

MAIN TEXT

The Arctic Ocean and its biota exhibit elevated levels of toxic mercury (Hg)[1] despite an absence of important local anthropogenic sources. Mercury is delivered to surface waters of the Arctic Ocean through atmospheric deposition, inputs from other oceans, riverine discharge, snow and sea ice melt[2]. High inputs of mainly inorganic mercury (iHg) coincide with the Arctic's biologically active summer season[3]. However, data on inter- and intra-seasonal Hg concentrations in the Arctic Ocean, especially during the winter, is lacking so far. The discovery of springtime atmospheric Hg depletion events[4] over 20 years ago highlighted a distinct seasonal aspect to Hg biogeochemical

cycling in the Arctic. Recently, increased attention on pan-Arctic rivers have also confirmed riverine Hg inputs to the Arctic shelf seas during spring flood events[5]. With increasing evidence of a highly seasonal Arctic Hg cycle, a lack of seawater observations in winter indicates that the current paradigm of the Arctic Ocean Hg budget and fluxes are only a "summer snapshot".

The seasonal transition from summer to winter in the Arctic Ocean is marked by decreased biological activity, weakened stratification, and sea ice growth. However, our understanding of Hg cycling during the Arctic winter is still largely based on assumptions with considerable uncertainty. Biogeochemical models suggest that water mixing during autumn resupplies Hg to upper waters[6]. The presence of sea ice restricts Hg exchange with the atmosphere[7] throughout autumn and winter, allowing potential buildup of gaseous mercury and dimethylmercury (DMHg) under sea ice[8]. As temperatures rise and light returns, sea ice melt and atmospheric inputs may explain increased springtime Hg concentrations in polar waters compared to winter Hg concentrations[9]. The spring freshet delivers additional Hg to surface waters from the major pan-Arctic rivers[10]. As a result, summer Hg observations in Arctic surface waters are elevated compared to deeper waters[11].

Arctic surface waters lose significant amounts of Hg via atmospheric evasion or scavenging with sinking particles. During the summer, photochemical reduction of riverine Hg and subsequent evasion emits a significant fraction of gaseous Hg back to the atmosphere[12]. However, recent observations indicate low Hg evasion to the atmosphere in late summer and autumn[8], suggesting particle scavenging dominates Hg losses from surface waters in autumn and winter. In addition, Arctic summer and autumn exhibit the highest total particulate matter fluxes due to peak primary

productivity[13,14]. Although particle fluxes decline in winter, dissolved Hg has a high affinity to particles due to high partitioning coefficients (K_D)[15]. Previous observations, models, and budgets[2,12,16-19] have hinted at the importance of scavenging of Hg on the shelf yet lack confirmation, especially during winter.

Seasonal loss of Hg on the Arctic shelves

We investigated a shelf to deep basin meridional transect in the northern Barents Sea in August – summer, and December – winter (Fig. 1). We sampled seawater for unfiltered total Hg (THg), the sum of all inorganic and organic Hg species, including both particulate and dissolved. We also collected seawater for unfiltered methylated mercury (MeHg), the sum of organic Hg species, monomethylmercury (MMHg) and DMHg.

Average THg concentrations (Fig. 2) in summer are 0.63 ± 0.19 pmol L^{-1} (range: 0.38 – 1.36 pmol L^{-1}, n = 60) and show a scavenged-type profile, similar to THg observations on previous summertime Arctic expeditions[16,17,20-23]. Our total Hg concentrations on the shelf (< 400 m depth, P1 – P5) are slightly higher and more variable compared to the shelf break (P6) and Nansen Basin (P7) stations (Fig. 2). We measured the highest THg concentrations in the polar mixed layer (< 20 m) under the sea ice. The higher Hg concentrations are most likely from Hg contained in pico- and nanophytoplankton in addition to Hg input from melting sea ice. Elevated surface THg concentrations in the southerly open water stations (P1 – P3) might also suggest atmospheric deposition[24]. Average THg concentrations on our transect trend lower than the Canadian Archipelago and the Siberian shelf seas[25], although this difference may be explained by the region's lack of major riverine sources and mixing of Hg-depleted Atlantic Water[17] and Hg-enriched Polar Water[11,26,27].

Our average THg concentrations in winter (Fig. 2) are 0.46 ± 0.07 pmol L^{-1} (range: 0.34 – 0.66 pmol L^{-1}, n = 61) and display less variability than summer concentrations (range: 0.38 – 1.36 pmol L^{-1}). The THg concentrations in the stratified Nansen Basin (P7) continue to exhibit a scavenged-type profile, while THg concentrations on the shelf stations (P1 – P5) have changed to a more conservative-type profile. Average winter THg concentrations at shelf stations (P1 – P5) including all sampled depths were 28 – 41% less than summer. Our overall average winter THg concentrations are similar to summer THg concentrations in Atlantic Water (0.43 ± 0.14 pmol L^{-1})[17] yet less variable. However, all shelf stations except P1 retain Polar Water signatures with additional sea ice cover. Colder and saltier surface waters in winter display weaker stratification and suggest mixing throughout the autumn (Extended Data Figs. 1 and 2). Therefore, our lower winter THg concentrations in surface waters suggest THg is not resupplied from subsurface waters during autumn as previously thought. Weak stratification and mixing promote downward transport of particles[28,29], where surface THg may be scavenged to deeper waters and sediments.

Seasonal scavenging of inorganic Hg

We investigated the scavenging dynamics of THg by calculating iHg (pmol L^{-1}), the difference between THg and MeHg concentrations at each discrete sampling depth. Temporal changes in iHg between summer and winter are represented as ΔiHg using the integrated seasonal difference between iHg concentrations at two depth intervals (Fig. 3). These calculated ΔiHg quantities indicate a gain or loss in the total iHg pool. Six stations (P1 – P6) showed a negative ΔiHg, or loss of iHg, by winter (Fig. 3). On average, ΔiHg was -208 ± 41 pmol m^{-2} d^{-1} in the upper 100 m on the shelf (P1 – P5). By taking the absolute value of ΔiHg, we can compare to directional fluxes. Our average |ΔiHg| on the shelf is comparable to recent estimates of particulate Hg fluxes (173 ± 78

pmol m^{-2} d^{-1}) using a radiotracer approach[19]. While particulate Hg is approximately 17% of THg concentrations in the Barents Sea shelf[19], our average seasonal iHg decrease of 39 – 50% in the upper 100 m (P1 – P5) suggests scavenging of both particulate and dissolved iHg species.

Previous work has suggested Hg shelf scavenging along the continental margins[30] driven by strong Hg-particle interactions. Updated estimates of Hg-particle partition coefficients (K_D) in the Arctic Ocean indicate high affinity to manganese and iron oxides[31]. We found high dissolved manganese (DMn) concentrations on the shelf in both summer and winter (Extended Data Fig. 3). Both DMn and total manganese (TMn, Extended Data Fig. 4) concentrations are highest near sediments[32] (Extended Data Figs. 3 – 5). Suboxic reducing conditions in shelf sediments supply Mn^{2+} to the overlying water column through mixing, sediment resuspension and diffusion[33]. Here, we speculate that seasonal decreases of DMn on the shelf in the upper 100 m (P1 – P5, Extended Data Figs. 3 and 6) are due to oxidation to insoluble MnO_2. Colloidal MnO_2 can form precipitates that can scavenge and shuttle iHg to deeper depths, similar to observations in the Baltic and the Black Seas[34]. In the absence of late summer POC fluxes, the DMn shuttle on the Arctic shelf may explain our seasonal losses of DMn (Extended Data Fig. 6), iHg (Fig. 3) and total lead (TPb, Extended Data Fig. 7). As TPb and THg have comparable K_D values for manganese particle phases in the Arctic Ocean[35], our negative ΔTPb values on shelf stations (P1 – P5, Extended Data Fig. 8) reflect similar trends to ΔiHg (Fig. 3). A seasonal loss of TPb on the Barents Sea shelf (P1 – P5) agrees well with previous hypotheses of strong Pb scavenging on the Arctic shelves[18,36-38].

Losses of gaseous Hg from Arctic surface waters may also influence our seasonal loss of iHg. We evaluated Hg^0 losses from summer to winter by limiting ΔiHg to the wind mixed layer (< 20 m).

We assumed our iHg concentrations at the shallowest sampling depth (approx. 10 m) were representative of the atmosphere-sea surface interface (0 m). Most stations (P1 – P6) exhibit a negative ΔiHg, with an average ΔiHg of -80 ± 14 pmol m^{-2} d^{-1} on the shelf (P1 – P5). By comparison, we calculated a net open water Hg^0 evasion rate of only 11 pmol m^{-2} d^{-1} from a late summer atmospheric evasion rate[8] combined with their suggested equal Hg inputs from deposition and meltwater. Accordingly, our low calculated Hg^0 evasion rate compared to high wind-mixed layer |ΔiHg| values suggest minimal losses of gaseous Hg species.

Persistent seawater MeHg

While THg concentrations showed significant seasonal differences, average MeHg concentrations remained constant (Fig. 4). Average summer MeHg concentrations were 0.11 ± 0.03 pmol L^{-1} (range; 0.08 – 0.23 pmol L^{-1}, n = 58) and winter concentrations were 0.12 ± 0.04 pmol L^{-1} (range; 0.07 – 0.23 pmol L^{-1}, n = 55). We found that MeHg concentrations exhibit near uniform distributions on the shelf (P1 – P5). In addition, a localized shallow MeHg maximum is seen at ~ 80 – 120 m depth in the Nansen Basin (P6 – P7), indicative of in situ MeHg production[16,17,21,23]. Below 200 m, MeHg at P6 and P7 displayed the typical profile of MeHg observed in the Fram Strait[17] with deeper maxima between 400 – 1000 m depth. Overall, both of our seasonal MeHg profiles are typical of the summer Arctic Ocean. Surprisingly, our unchanged seasonal MeHg profiles are in stark contrast to our seasonal THg profiles.

While it is difficult to estimate, one could expect seasonal changes of MeHg due to the absence of photochemistry[39], sea ice cover limiting evasion to the atmosphere[8], net demethylation[40] and low primary productivity during winter[3,41]. Similar to ΔiHg, we calculated ΔMeHg at each station by integrating the winter MeHg reservoir and comparing it to the integrated summer MeHg reservoir

at two depth intervals (Fig. 3). Our calculated ΔMeHg in the upper 100 m are small and show no clear trend (range: -25 to 15 pmol m^{-2} d^{-1}, SI Table 1). We expect waters to be in a net state of demethylation[40] as low particulate organic carbon (POC) fluxes on the shelf suggest minimal in situ production of MeHg[42]. As a result, small variations in our ΔMeHg therefore suggest seasonal MeHg distributions to be in a locally dynamic equilibrium.

On the other hand, our winter MeHg concentrations may remain the same as summer due to the absence of photodegradation[39,43]. Additionally, reduced losses of DMHg due to the presence of sea ice may also explain static winter MeHg concentrations, although MMHg is typically the dominant species on the shelf[17,23]. Particle scavenging can also transport MMHg to deeper waters and sediments, decreasing MeHg and THg concentrations in the water column. Higher amounts of gaseous DMHg, with negligible affinity to sinking particles, could also explain the persistence of MeHg concentrations. In addition, the K_D of MMHg may be an order of magnitude lower than THg[44], reducing its affinity to sinking particles and explaining the difference in our THg and MeHg trends. Generally, particulate MMHg concentrations in the Arctic Ocean are low, approximately 4% of MeHg[23]. Consequently, our unchanged MeHg concentrations therefore suggest high proportions of dissolved MeHg in both summer and winter.

Implications for the Arctic Hg cycle

The first observations during the polar night demonstrate a seasonal loss of THg. We suggest that the seasonal loss is primarily driven by particle scavenging of iHg via an Arctic DMn shuttle. Seasonal scavenging mechanisms on the entire Arctic shelf during the polar night may dominate water column Hg losses to shelf sediments. We also suggest MeHg concentrations are maintained in the water column in winter by reduced evasion, low particle affinities, slow demethylation rates

and a lack of photodegradation. Although in situ production is the dominant source of the subsurface MeHg maximum during summer in the Arctic basin, small shelf to basin transport of MeHg produced in the shelf sediments may contribute partially to the persistent shallow MeHg maximum and positive ΔMeHg seen in the Arctic basin (P7) in winter (Fig. 3 & 4). Assuming a shelf seasonal loss of 33 – 46% iHg including all sampled depths (P1 – P5), we estimate a residence time for iHg of ~ 3 years. However, the persistence of MeHg extends the lifetime of THg in the Arctic Ocean to ~ 9 years[17]. Our work highlights a potential decoupling of iHg and MeHg species during the polar night and invites a new seasonally based paradigm of the Arctic Hg budget.

In the future, climate change is expected to significantly affect the biogeochemical cycle of Hg[45,46] and drive MeHg concentrations in the marine food chain[47]. Sea ice loss will increase primary productivity on the Arctic shelves[48] and lead to greater iHg export to deeper waters and sediments. In addition, thawing permafrost and increased riverine flux will deliver high iHg inputs to the Arctic shelves. Recent work has suggested increased Hg uptake in benthic feeding-organisms on the Arctic shelf[49]. We anticipate that seasonal scavenging during autumn and winter months will deliver larger amounts of iHg to shelf sediments, driving increased benthic MeHg production and MeHg accumulation in the future Arctic Ocean.

CORRESPONDING AUTHOR STATEMENT

Correspondence and requests for materials should be addressed to SGK, stephen.g.kohler@ntnu.no, LEHB, lars-eric.heimburger@mio.osupytheas.fr or MVA, murat.v.ardelan@ntnu.no.

ACKNOWLEDGEMENTS

Financial support for this study was provided by the Norwegian University of Science and Technology (NTNU) (SGK) and the Research Council of Norway through The Nansen Legacy project, RCN#276730 (SGK, MGD, NS, MVA). We would like to thank the captain, crew, cruise leaders, and fellow scientists onboard *R/V Kronprins Haakon* on cruises Q3 and Q4. Additional thanks are to the entire Marine Biogeochemistry group at NTNU for their guidance and support. In addition, thanks to the Marseille Marine Mercury group and Marie-Maëlle Desgranges for her help with preparing the Hg samples for analysis.

AUTHOR CONTRIBUTIONS STATEMENT

SGK: Conceptualization, formal analysis, investigation, validation, visualization, writing – original draft. **LEHB:** Conceptualization, formal analysis, investigation, resources, writing – review and editing, supervision. **MVP:** Formal analysis, investigation, validation, resources, writing – review and editing. **MGD:** Investigation, writing – review and editing. **NS:** Formal analysis, investigation, writing – review and editing. **AD:** Formal analysis, validation, writing – review and editing. **AS:** Formal analysis, validation, writing – review and editing. **KN:** Conceptualization, writing – review and editing, supervision. **MVA:** Conceptualization, investigation, resources, writing – review and editing, supervision, funding acquisition.

COMPETING INTERESTS STATEMENT

The authors declare no competing interests.

FIGURE LEGENDS/CAPTIONS

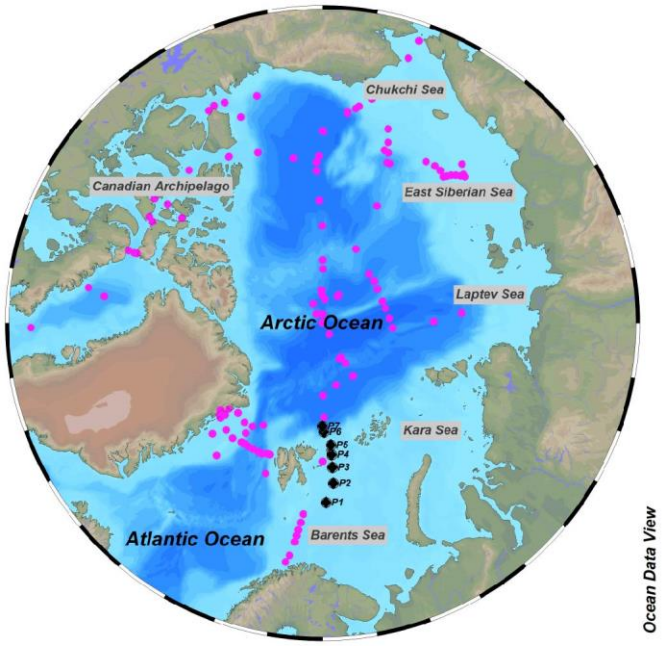

Figure 1: Map of water column Hg profiles in the Arctic Ocean. Literature data marked with pink circles[1,16,17,20,21,23,25,50]. Stations (P1 – P7), sampled during the 2019 summer and winter cruises, marked with black diamonds.

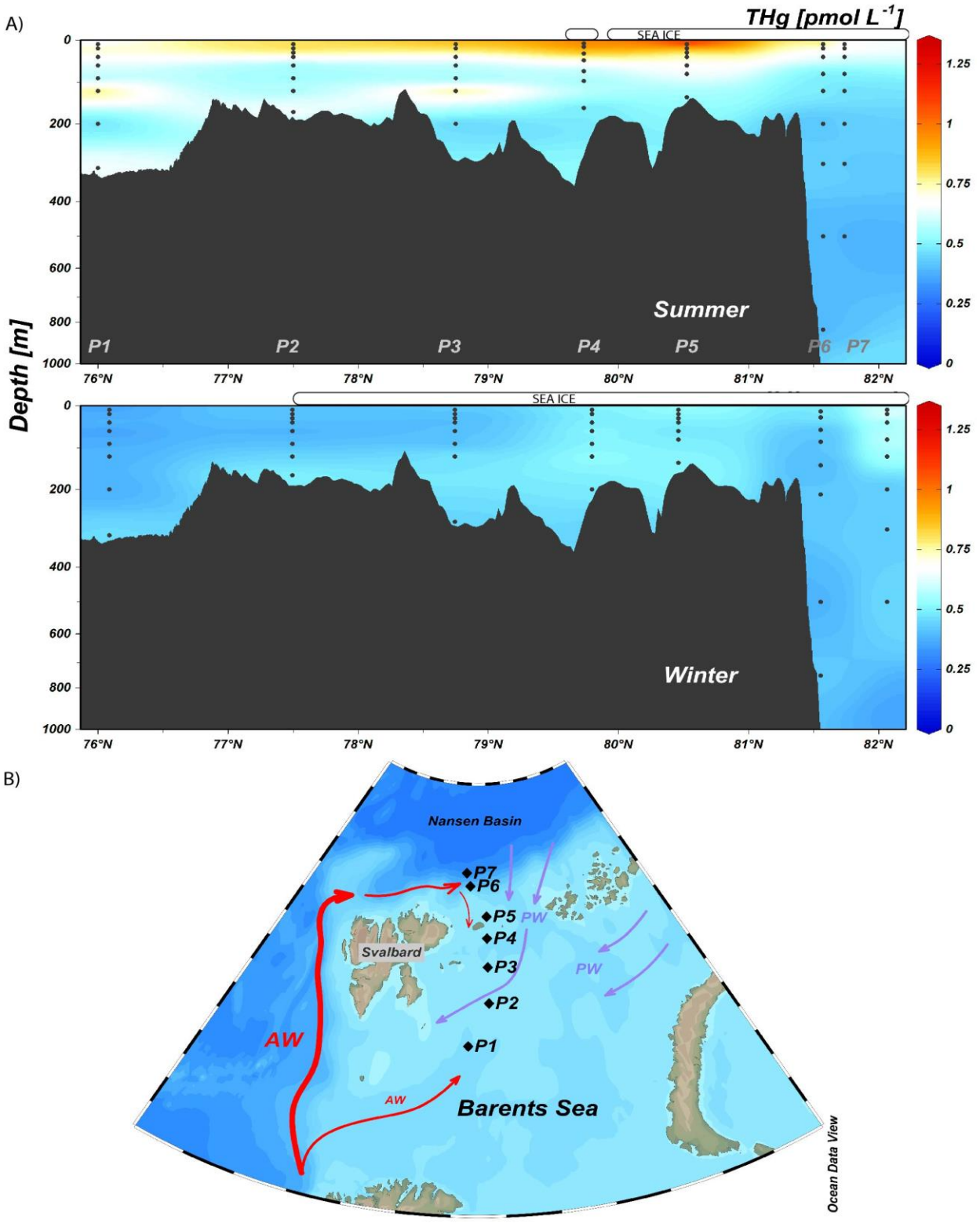

Figure 2: Total mercury (THg) concentrations (pmol L^{-1}) along the shelf-deep basin gradient.

A) Stations P1 – P7, (Latitude) are on the x-axis for summer 2019 and winter 2019 cruises. B)

Map of sampling stations with warmer Atlantic Water (AW) advected into the Barents Sea from the south and west, and Polar Water (PW) advected from the north and east[27].

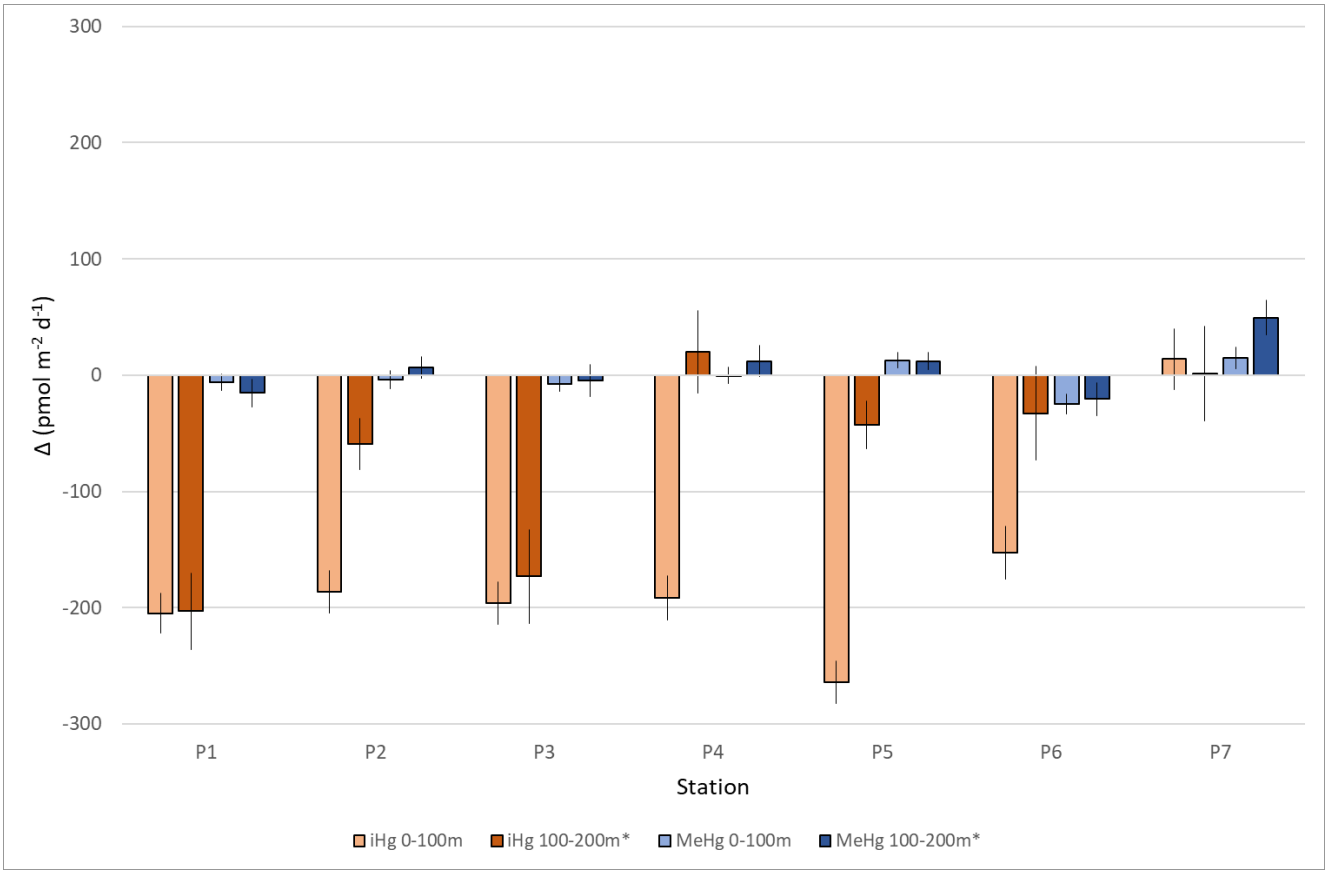

Figure 3: ΔiHg (pmol m^{-2} d^{-1}) and ΔMeHg (pmol m^{-2} d^{-1}) at specified depth intervals for each station. iHg 0-100 m is in light orange, iHg 100-200 m in dark orange, MeHg 0-100 m in light blue, and MeHg 100-200 m in dark blue. A positive Δ value indicates a temporal gain in the iHg or MeHg pool while a negative Δ value indicates a temporal loss in the iHg or MeHg pool. Error bars represent combined standard uncertainty (±1σ). Values associated with Figure 3 are compiled in SI Table 1. *Stations P2 and P5 were integrated from 100 m to sample depth less than 200 m.

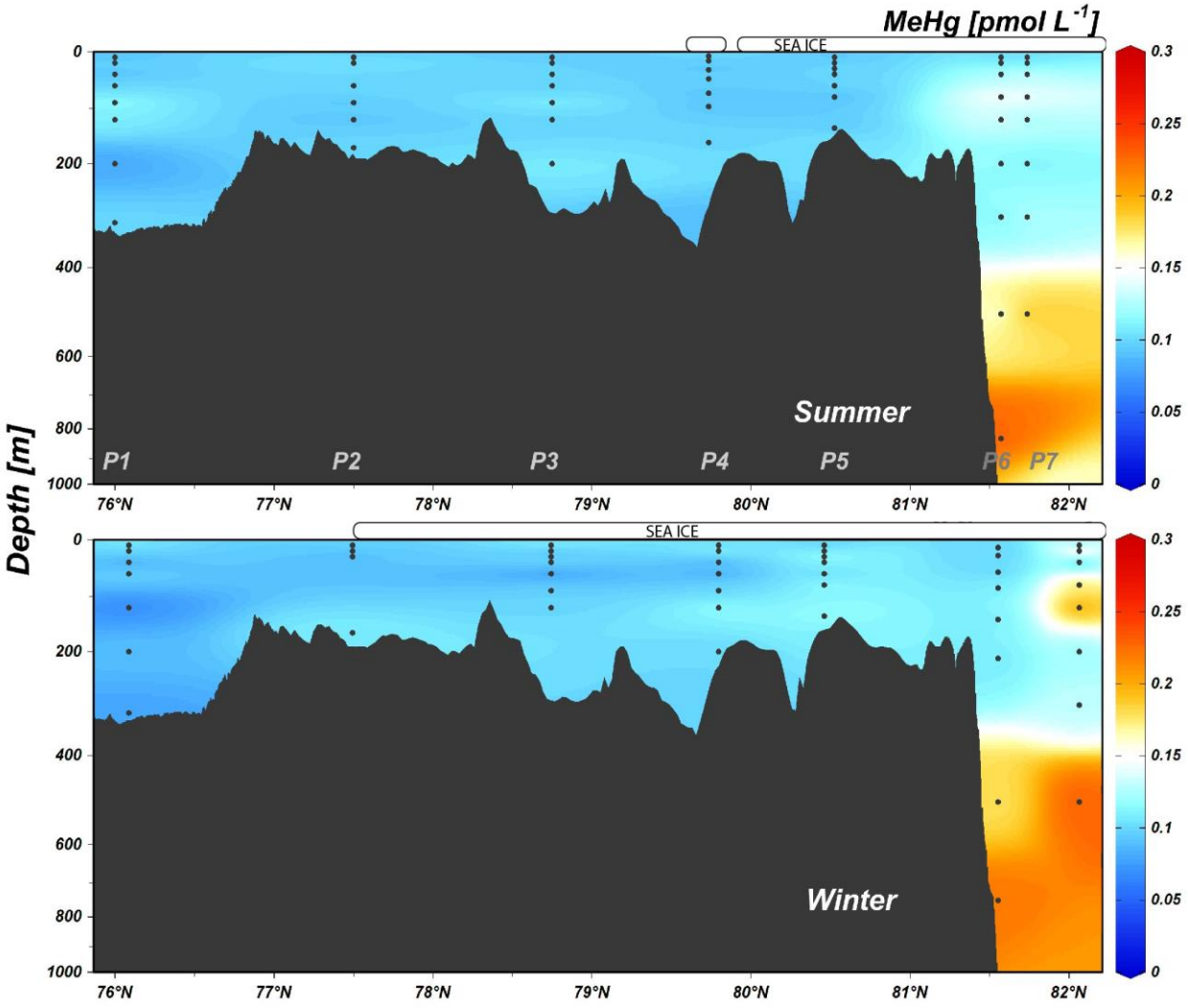

Figure 4: Total methylated mercury (MeHg) concentrations (pmol L^{-1}) along the shelf-deep basin gradient. Stations P1 – P7, (Latitude) are on the x-axis for summer 2019 (top) and winter 2019 cruises (bottom).

REFERENCES

1 Wang, K. *et al.* Subsurface seawater methylmercury maximum explains biotic mercury concentrations in the Canadian Arctic. *Sci Rep* **8**, 14465, (2018).

2 Soerensen, A. L. *et al.* A mass budget for mercury and methylmercury in the Arctic Ocean. *Global Biogeochemical Cycles* **30**, 560-575, (2016).

3 Wassmann, P. Arctic marine ecosystems in an era of rapid climate change. *Progress in Oceanography* **90**, 1-17, (2011).

4 Schroeder, W. H. *et al.* Arctic springtime depletion of mercury. *Nature* **394**, 331-332, (1998).

5 Sonke, J. E. *et al.* Eurasian river spring flood observations support net Arctic Ocean mercury export to the atmosphere and Atlantic Ocean. *Proc Natl Acad Sci U S A* **115**, E11586-E11594, (2018).

6 Fisher, J. A. *et al.* Riverine source of Arctic Ocean mercury inferred from atmospheric observations. *Nat Geosci* **5**, 499-504, (2012).

7 Andersson, M. E., Sommar, J., Gårdfeldt, K. & Lindqvist, O. Enhanced concentrations of dissolved gaseous mercury in the surface waters of the Arctic Ocean. *Marine Chemistry* **110**, 190-194, (2008).

8 DiMento, B. P., Mason, R. P., Brooks, S. & Moore, C. The impact of sea ice on the air-sea exchange of mercury in the Arctic Ocean. *Deep-Sea Res Pt I* **144**, 28-38, (2019).

9 Nerentorp Mastromonaco, M. G., Gårdfeldt, K., Langer, S. & Dommergue, A. Seasonal Study of Mercury Species in the Antarctic Sea Ice Environment. *Environ Sci Technol* **50**, 12705-12712, (2016).

10 Zolkos, S. *et al.* Mercury Export from Arctic Great Rivers. *Environ Sci Technol* **54**, 4140-4148, (2020).

11 Bowman, K. L., Lamborg, C. H. & Agather, A. M. A global perspective on mercury cycling in the ocean. *Sci Total Environ* **710**, 136166, (2020).

12 Zhang, Y. *et al.* Biogeochemical drivers of the fate of riverine mercury discharged to the global and Arctic oceans. *Global Biogeochemical Cycles* **29**, 854-864, (2015).

13 Nöthig, E. M. *et al.* Summertime Chlorophyll a and Particulate Organic Carbon Standing Stocks in Surface Waters of the Fram Strait and the Arctic Ocean (1991–2015). *Frontiers in Marine Science* **7**, 350, (2020).

14 Nöthig, E. M. *et al.* Annual cycle of downward particle fluxes on each side of the Gakkel Ridge in the central Arctic Ocean. *Philos Trans A Math Phys Eng Sci* **378**, 20190368, (2020).

15 Lamborg, C. H., Hammerschmidt, C. R. & Bowman, K. L. An examination of the role of particles in oceanic mercury cycling. *Philos Trans A Math Phys Eng Sci* **374**, 20150297, (2016).

16 Wang, F., Macdonald, R. W., Armstrong, D. A. & Stern, G. A. Total and methylated mercury in the Beaufort Sea: the role of local and recent organic remineralization. *Environ Sci Technol* **46**, 11821-11828, (2012).

17 Petrova, M. V. *et al.* Mercury species export from the Arctic to the Atlantic Ocean. *Marine Chemistry* **225**, 103855, (2020).

18 Charette, M. A. *et al.* The Transpolar Drift as a Source of Riverine and Shelf-Derived Trace Elements to the Central Arctic Ocean. *J Geophys Res-Oceans* **125**, e2019JC015920, (2020).

19 Tesán, J. *et al.* Mercury export flux in the Arctic Ocean estimated from 234Th: 238U disequilibria. *ACS Earth and Space Chemistry* **4**, 795-801 (2020).

20 Kirk, J. L. *et al.* Methylated mercury species in marine waters of the Canadian high and sub Arctic. *Environ Sci Technol* **42**, 8367-8373, (2008).

21 Heimbürger, L. E. *et al.* Shallow methylmercury production in the marginal sea ice zone of the central Arctic Ocean. *Sci Rep* **5**, 1-6, (2015).

22 Cossa, D. *et al.* Sources, cycling and transfer of mercury in the Labrador Sea (GEOTRACES-GEOVIDE cruise). *Marine Chemistry* **198**, 64-69, (2018).

23 Agather, A. M., Bowman, K. L., Lamborg, C. H. & Hammerschmidt, C. R. Distribution of mercury species in the Western Arctic Ocean (US GEOTRACES GN01). *Marine Chemistry* **216**, 103686, (2019).

24 Hirdman, D. *et al.* Transport of mercury in the Arctic atmosphere: Evidence for a spring-time net sink and summer-time source. *Geophysical Research Letters* **36**, L12814, (2009).

25 Kim, J. *et al.* Mass Budget of Methylmercury in the East Siberian Sea: The Importance of Sediment Sources. *Environ Sci Technol* **54**, 9949-9957, (2020).

26 Loeng, H. Features of the Physical Oceanographic Conditions of the Barents Sea. *Polar Research* **10**, 5-18, (1991).

27 Sundfjord, A., Assmann, K.M, Lundesgaard, Ø., Renner, A.H.H, & Ingvaldsen, R.B. Suggested water mass defintions for the central and northern Barents Sea, and the adjacent Nansen Basin: Workshop Report. *The Nansen Legacy Report Series* **8**, (2020).

28 Olli, K. *et al.* Seasonal variation in vertical flux of biogenic matter in the marginal ice zone and the central Barents Sea. *Journal of Marine Systems* **38**, 189-204, (2002).

29 Reigstad, M., Riser, C. W., Wassmann, P. & Ratkova, T. Vertical export of particulate organic carbon: Attenuation, composition and loss rates in the northern Barents Sea. *Deep-Sea Research Part II-Topical Studies in Oceanography* **55**, 2308-2319, (2008).

30 Cossa, D., Cotté-Krief, M. H., Mason, R. P. & Bretaudeau-Sanjuan, J. Total mercury in the water column near the shelf edge of the European continental margin. *Marine Chemistry* **90**, 21-29, (2004).

31 Cui, X., Lamborg, C. H., Hammerschmidt, C. R., Xiang, Y. & Lam, P. J. The Effect of Particle Composition and Concentration on the Partitioning Coefficient for Mercury in Three Ocean Basins. *Frontiers in Environmental Chemistry* **2**, 6, (2021).

32 Middag, R., de Baar, H. J. W., Laan, P. & Klunder, M. B. Fluvial and hydrothermal input of manganese into the Arctic Ocean. *Geochimica Et Cosmochimica Acta* **75**, 2393-2408, (2011).

33 Vieira, L. H. *et al.* Benthic fluxes of trace metals in the Chukchi Sea and their transport into the Arctic Ocean. *Marine Chemistry* **208**, 43-55, (2019).

34 Rosati, G. *et al.* Mercury in the Black Sea: New Insights From Measurements and Numerical Modeling. *Global Biogeochem Cycles* **32**, 529-550, (2018).

35 Bam, W. *et al.* Variability in 210Pb and 210Po partition coefficients (Kd) along the US GEOTRACES Arctic transect. *Marine Chemistry* **219**, 103749, (2020).

36 Smith, J. N., Moran, S. B. & Macdonald, R. W. Shelf–basin interactions in the Arctic Ocean based on 210Pb and Ra isotope tracer distributions. *Deep Sea Research Part I: Oceanographic Research Papers* **50**, 397-416, (2003).

37 Lepore, K., Moran, S. B. & Smith, J. N. 210Pb as a tracer of shelf–basin transport and sediment focusing in the Chukchi Sea. *Deep Sea Research Part II: Topical Studies in Oceanography* **56**, 1305-1315, (2009).

38 Kadko, D. *et al.* The residence times of trace elements determined in the surface Arctic Ocean during the 2015 US Arctic GEOTRACES expedition. *Marine Chemistry* **208**, 56-69, (2019).

39 Point, D. *et al.* Methylmercury photodegradation influenced by sea-ice cover in Arctic marine ecosystems. *Nat Geosci* **4**, 188-194, (2011).

40 Lehnherr, I., St Louis, V. L., Hintelmann, H. & Kirk, J. L. Methylation of inorganic mercury in polar marine waters. *Nat Geosci* **4**, 298-302, (2011).

41 Heimbürger, L. E. *et al.* Methyl mercury distributions in relation to the presence of nano- and picophytoplankton in an oceanic water column (Ligurian Sea, North-western Mediterranean). *Geochimica et Cosmochimica Acta* **74**, 5549-5559, (2010).

42 Sunderland, E. M., Krabbenhoft, D. P., Moreau, J. W., Strode, S. A. & Landing, W. M. Mercury sources, distribution, and bioavailability in the North Pacific Ocean: Insights from data and models. *Global Biogeochemical Cycles* **23**, GB2010, (2009).

43 Seller, P., Kelly, C. A., Rudd, J. W. M. & MacHutchon, A. R. Photodegradation of methylmercury in lakes. *Nature* **380**, 694-697, (1996).

44 Lawson, N. M., Mason, R. P. & Laporte, J. M. The fate and transport of mercury, methylmercury, and other trace metals in Chesapeake Bay tributaries. *Water Res* **35**, 501-515, (2001).

45 Stern, G. A. *et al.* How does climate change influence Arctic mercury? *Sci Total Environ* **414**, 22-42, (2012).

46 Krabbenhoft, D. P. & Sunderland, E. M. Environmental science. Global change and mercury. *Science* **341**, 1457-1458, (2013).

47 Schartup, A. T. *et al.* Climate change and overfishing increase neurotoxicant in marine predators. *Nature* **572**, 648-650, (2019).

48 Arrigo, K. R. & van Dijken, G. L. Continued increases in Arctic Ocean primary production. *Progress in Oceanography* **136**, 60-70, (2015).

49 Gopakumar, A., Giebichenstein, J., Raskhozheva, E. & Borgå, K. Mercury in Barents Sea fish in the Arctic polar night: Species and spatial comparison. *Mar Pollut Bull* **169**, 112501, (2021).

METHODS

Sample collection

The transect in the northern Barents Sea and Nansen Basin (76°N – 83°N) was sampled on two cruises, Q3 and Q4, in August 2019 and December 2019 on *R/V Kronprins Haakon* as part of The Nansen Legacy project. Water samples were collected manually using Teflon-coated GOFLO bottles attached sequentially to a 600 m Aramid rope. Seawater was sampled at seven stations at 8 depths up to 500 m. Depths deeper than 500 m were sampled with 10 L Niskin bottles mounted to a rosette with a SeaBird SBE 9 CTD unit. Upon GOFLO retrieval, bottles were transported immediately to an onboard custom-made clean lab. High-efficiency particulate air filter cartridges were attached to the pressure release valve. THg samples were collected unfiltered with no headspace into pre-cleaned[51] 40 mL borosilicate glass bottles with PTFE-lined caps and kept unpreserved. MeHg samples were collected unfiltered into brand new 125 mL PET bottles and were acidified to 0.4 % v/v double-distilled HCl under a Class 100 clean air laminar flow hood. Upon acidification, dimethylmercury (DMHg) converts quantitatively to monomethylmercury (MMHg)[52]; thus, total methylated mercury (MeHg) is measured as the sum of MMHg and DMHg. All samples were double-bagged and stored in the dark at 4°C until analysis.

Hg measurements

The THg concentration in the samples was measured according to USEPA Method 1631 at the Mediterranean Institute of Oceanography (MIO) using a custom-made single gold trap setup described elsewhere[21] within six months after sampling. To adapt to the low concentrations expected in seawater, potassium bromide (Sigma Aldrich, USA) and potassium bromate (Sigma Aldrich, USA) are heated for 4h at 250°C to remove Hg traces before making up BrCl solution

with freshly double-distilled HCl. The BrCl solution was blank checked prior to use using a standard addition protocol. Field blanks were measured for both summer (0.01 pmol L^{-1}, n = 4) and winter (0.09 pmol L^{-1}, n = 3) cruises. Average THg concentrations are reported in the main text plus the standard deviation of the mean (±1SD).

THg measurements were calibrated against NIST 3133 (National Institute of Standards and Technology), with a 6-point calibration curve in Hg-free seawater (R^2 values of 0.9998 – 1), accounting for matrix effects. A NIST quality control sample was spiked into previously purged Hg-free sample seawater matrix and analyzed after every 6 samples (standard-bracketing) to monitor instrumental drift. Initial recovery and precision of this quality control sample for our batches is 94 ± 7%. Ongoing recovery of this quality control sample was monitored and checked against the recovery guidelines outlined in EPA Method 1631, Revision E, Table 2 (77 – 123%). The detection limit of 0.003 pmol L^{-1} was evaluated as 3x the standard deviation of the instrumental CVAFS "bubbler" blank. To test our analytical method, certified reference materials ORMS-5 and BCR-579 were spiked into previously purged Hg-free seawater matrix to test for recovery. Both standards were within the certified ranges, with additional analytical details provided in Supplemental Information.

The MeHg concentration in seawater samples was measured using the isotope dilution (ID) technique via gas chromatography – sector field ICP-MS (GC-SF-ICP-MS)[21] at MIO within six months after sampling. Briefly, enriched isotopic spikes of $i^{199}Hg$ and $MM^{201}Hg$ (ISC Science) were added to approximately 110 mL of seawater sample in pre-combusted borosilicate glass bottles and equilibrated for 15 minutes. Samples were adjusted to pH 3.9 using a sodium acetate

buffer solution (ULTREX® II Ultrapure Reagent, J.T. Baker, USA) and NH_3 (ULTREX® II Ultrapure Reagent, J.T. Baker, USA). A freshly made 1% solution of sodium tetrapropylborate (Merseburger Spezialchemikalien) and 200 µL of hexane (Sigma Aldrich) were added to derivatize and extract Hg species. Bottles were sealed and shaken for 15 minutes before the organic layer was transferred to GC vials for injection on a coupled GC (THERMO GC 1300 with GC220 transfer module) SF-ICP-MS (Thermo Element XR) system. The coupling to a high resolution ICP-MS and application of ultra-trace clean techniques allows reaching a detection limit of 0.001 pmol L^{-1}. We determined that the accuracy of our $MM^{201}Hg$ spike concentration compared to its theoretical concentration was 96.6 ± 7.9%, calculated with reverse isotope dilution using the Brooks Rand MeHgCl standard, traceable to NIST1641E. Additional analytical details are provided in Supplemental Information. Average MeHg concentrations are reported in the main text plus the standard deviation of the mean (±1SD).

Δ calculations

We calculate iHg for each depth as the difference between THg and MeHg. iHg and MeHg in the upper 200 m water column at each station were depth integrated using the trapezoidal method. ΔMeHg (Equation 1) and ΔiHg (Equation 2) were calculated from summer (s) to winter (w) using the specific sampling dates. We assumed the same concentrations of THg and MeHg at 0 m until observations begin at 10 m. When sampling depths differ or are missing, concentrations were extrapolated by linear regression from the closest available sampling depths to calculate Δ values.

$$\Delta MeHg = \left(\int_0^z [MeHg]_s dz - \int_0^z [MeHg]_w dz\right) / dt \quad (1)$$

$$\Delta iHg = \left(\int_0^z ([THg]_s - [MeHg]_s) dz - \int_0^z ([THg]_w - [MeHg]_w) dz\right) / dt \quad (2)$$

A positive Δ value indicates a temporal gain in iHg and MeHg while a negative Δ value indicates a temporal loss in iHg and MeHg. To compare directly to published fluxes, we present absolute values of ΔiHg and ΔMeHg as |ΔiHg| and |ΔMeHg|. Uncertainty in Δ values is reported as combined standard uncertainty (±1σ) calculated from the uncertainty in measured THg concentrations and uncertainty in measured MeHg concentrations.

Data availability statement

Figures 1, 2, and 4 and Extended Data Figures 1-5 and 7 were created by the publicly available Ocean Data View[55] and edited in Adobe Illustrator. Temperature and salinity data from seasonal cruises are publicly available from the Norwegian Marine Data Centre (https://nmdc.no)[53,54]. Mercury and trace element concentration data for all depths and stations are publicly available from the Norwegian Marine Data Centre (https://nmdc.no)[56,57]. Figure 3 and Extended Data Figures 6 and 8 were created in Microsoft Excel with data displayed in Supplementary Tables 1 and 3.

References

50 GEOTRACES Intermediate Data Product Group (2021). The GEOTRACES Intermediate Data Product 2021 (IDP2021). NERC EDS British Oceanographic Data Centre NOC. DOI: 10.5285/cf2d9ba9-d51d-3b7c-e053-8486abc0f5fd .

51 Hammerschmidt, C. R., Bowman, K. L., Tabatchnick, M. D. & Lamborg, C. H. Storage bottle material and cleaning for determination of total mercury in seawater. *Limnol Oceanogr-Meth* **9**, 426-431, (2011).

52 Black, F. J., Conaway, C. H. & Flegal, A. R. Stability of dimethyl mercury in seawater and its conversion to monomethyl mercury. *Environ Sci Technol* **43**, 4056-4062, (2009).

53 Reigstad, M. CTD data from Nansen Legacy Cruise - Seasonal cruise Q3. Norwegian Marine Data Centre https://doi.org/10.21335/NMDC-1107597377 (2022).

54 Søreide, J. CTD data from Nansen Legacy Cruise - Seasonal cruise Q4. Norwgian Marine Data Centre https://doi.org/10.21335/NMDC-301551919 (2022).

55 Schlitzer, R. Ocean Data View. odv.awi.de (2021).

56 Kohler, S. G. *et al.* Concentrations of total mercury, total methylated mercury, and selected trace elements in the northern Barents Sea as part of the Nansen Legacy project, Cruise 2019706 Q3. Norwegian Marine Data Centre https://doi.org/10.21335/NMDC-416151559 (2022).

57 Kohler, S. G. *et al.* Concentrations of total mercury, total methylated mercury, and selected trace elements in the northern Barents Sea as part of the Nansen Legacy project, Cruise 2019711 Q4. Norwegian Marine Data Centre https://doi.org/10.21335/NMDC-1871554897 (2022).

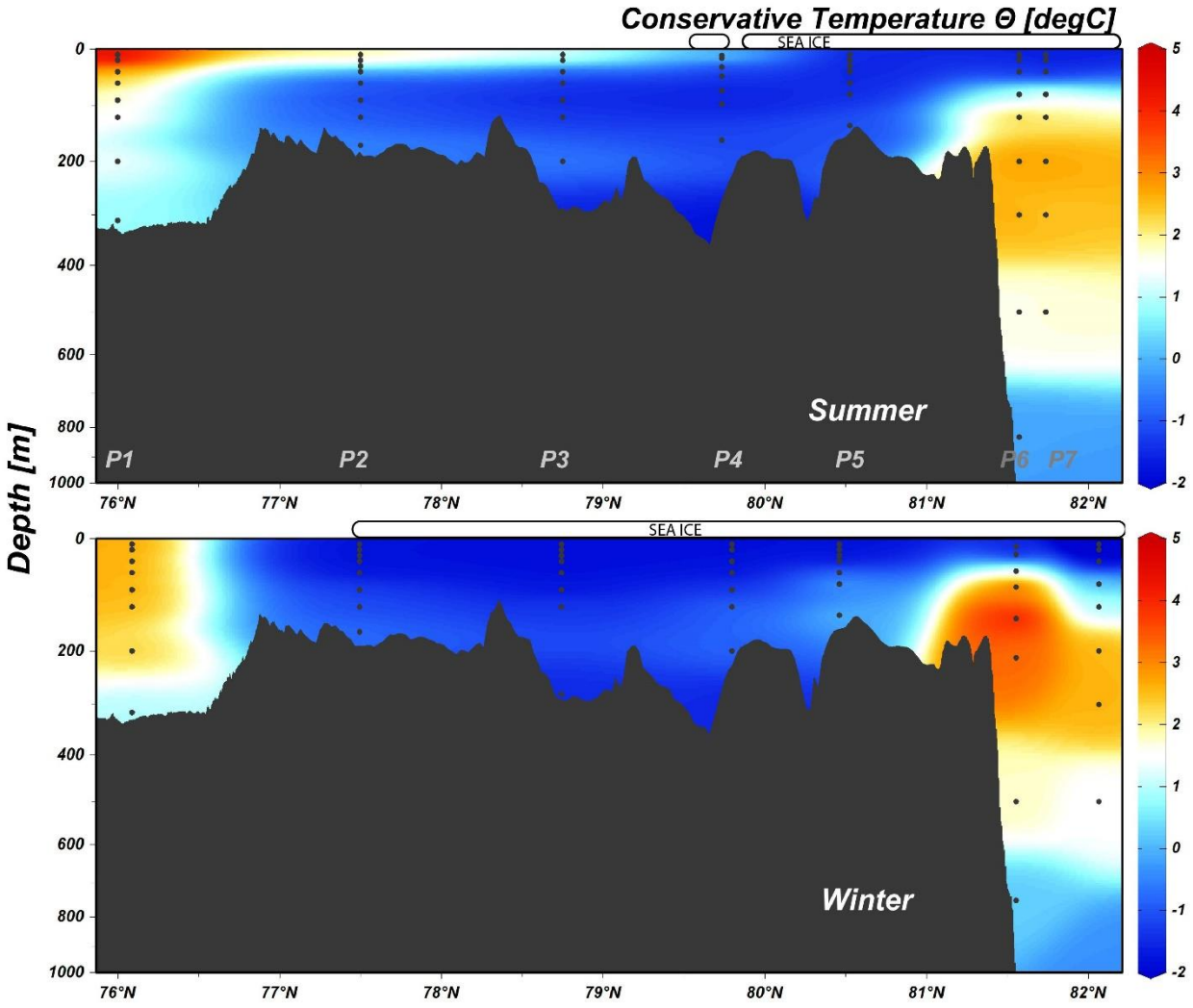

Extended Data Fig. 1. Conservative temperature (Θ) in degrees Celsius (°C) along the shelf-deep basin gradient. Stations P1 – P7, (Latitude) are on the x-axis for summer 2019 (top) and winter 2019 cruises (bottom). Data retrieved from the Norwegian Marine Data Centre[53,54].

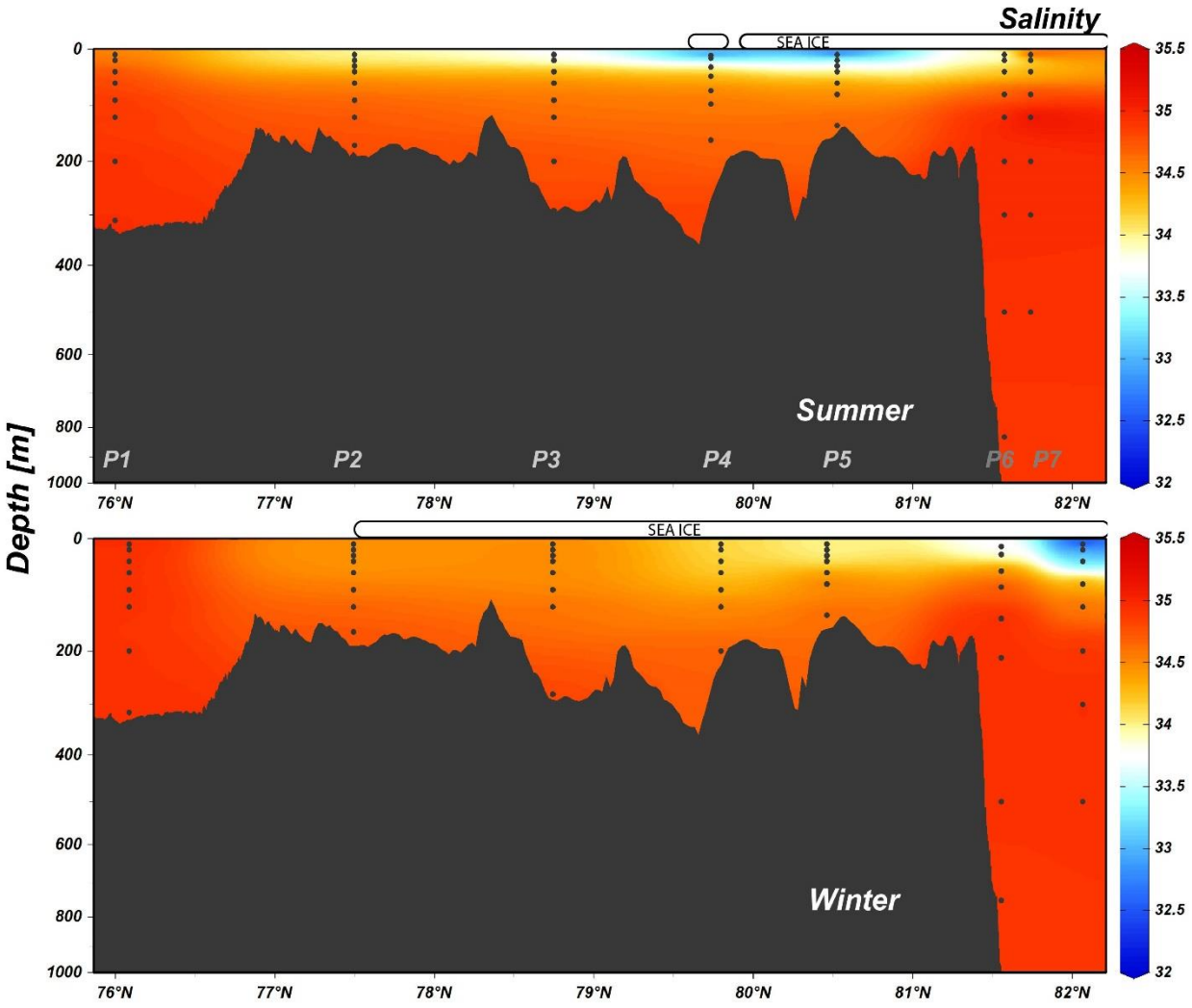

482

483 **Extended Data Fig. 2. Salinity along the shelf-deep basin gradient.** Stations P1 – P7, (Latitude)
484 are on the x-axis for summer 2019 (top) and winter 2019 cruises (bottom). Data retrieved from the
485 Norwegian Marine Data Centre[53,54.]

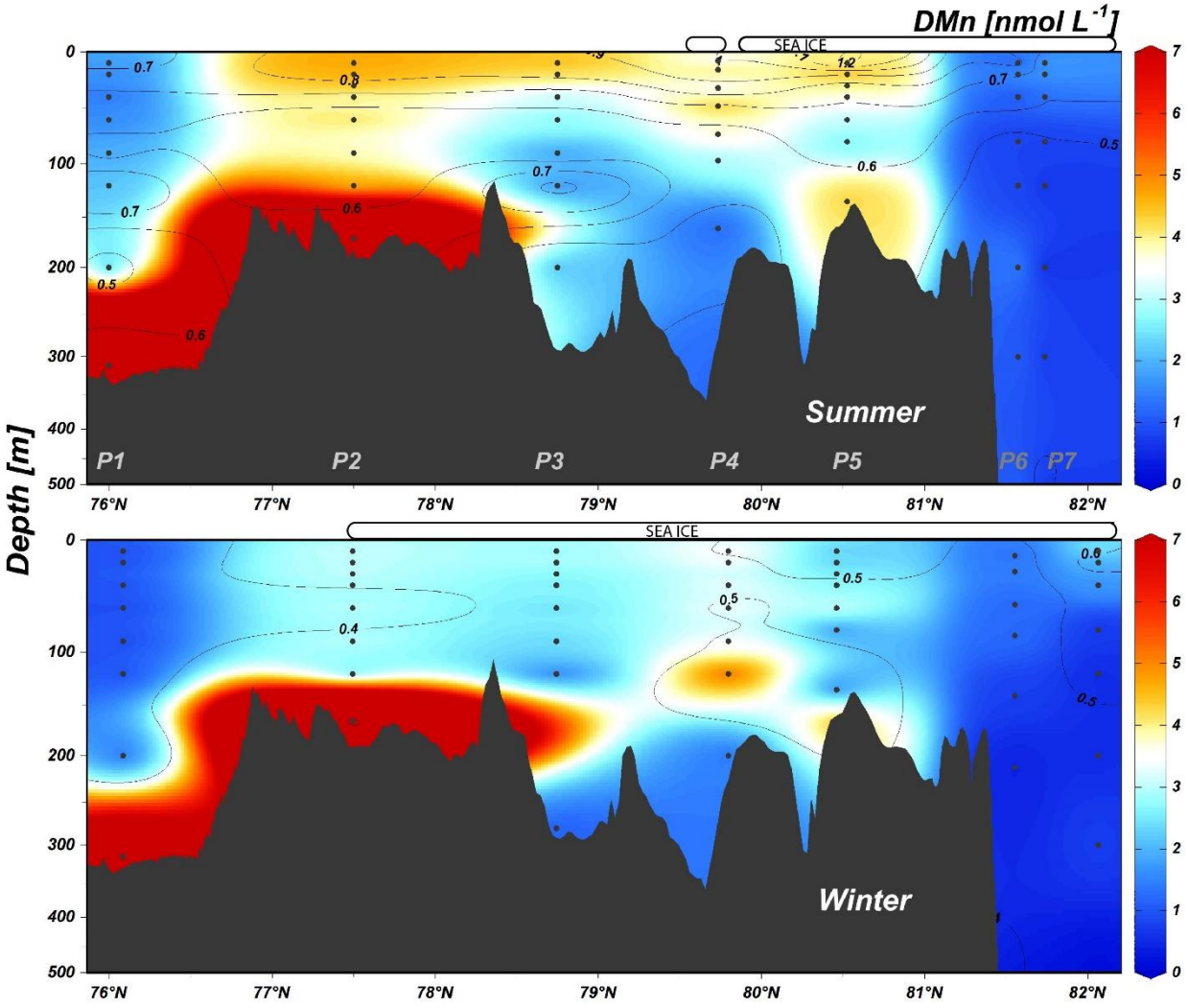

Extended Data Fig. 3. Dissolved manganese (DMn) concentrations (nmol L^{-1}) along the shelf-deep basin gradient. Stations P1 – P7, (Latitude) are on the x-axis for summer 2019 (top) and winter 2019 cruises (bottom). Black contour lines for THg (pmol L^{-1}) from each corresponding season are overlain. Concentrations greater than the presented range (7 nmol L^{-1}) are plotted as the maximum.

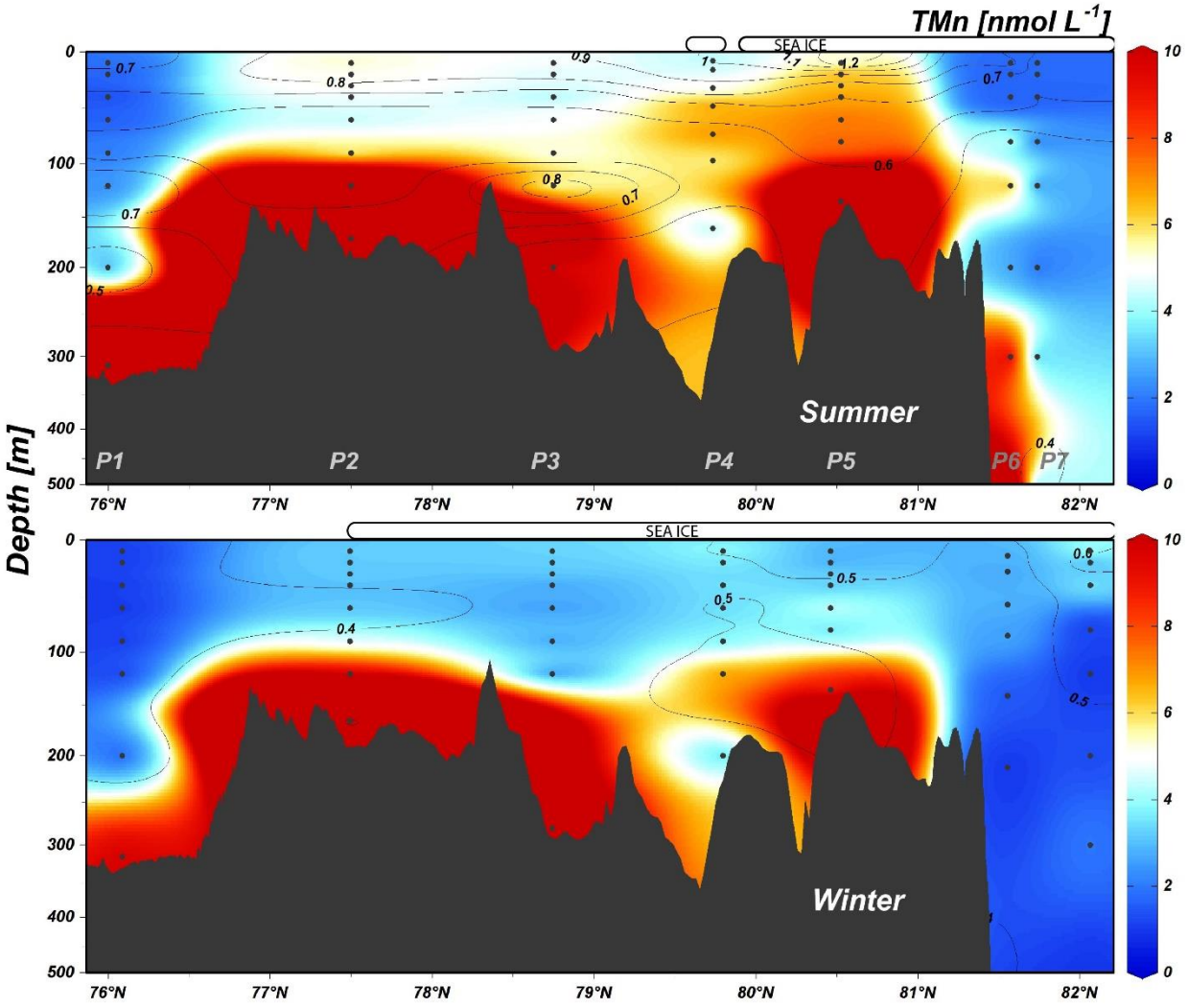

Extended Data Fig. 4. Total acid-leachable manganese (TMn) concentrations (nmol L^{-1}) along the shelf-deep basin gradient. Stations P1 – P7, (Latitude) are on the x-axis for summer 2019 (top) and winter 2019 cruises (bottom). Black contour lines for THg (pmol L^{-1}) from each corresponding season are overlain. Concentrations greater than the presented range (10 nmol L^{-1}) are plotted as the maximum.

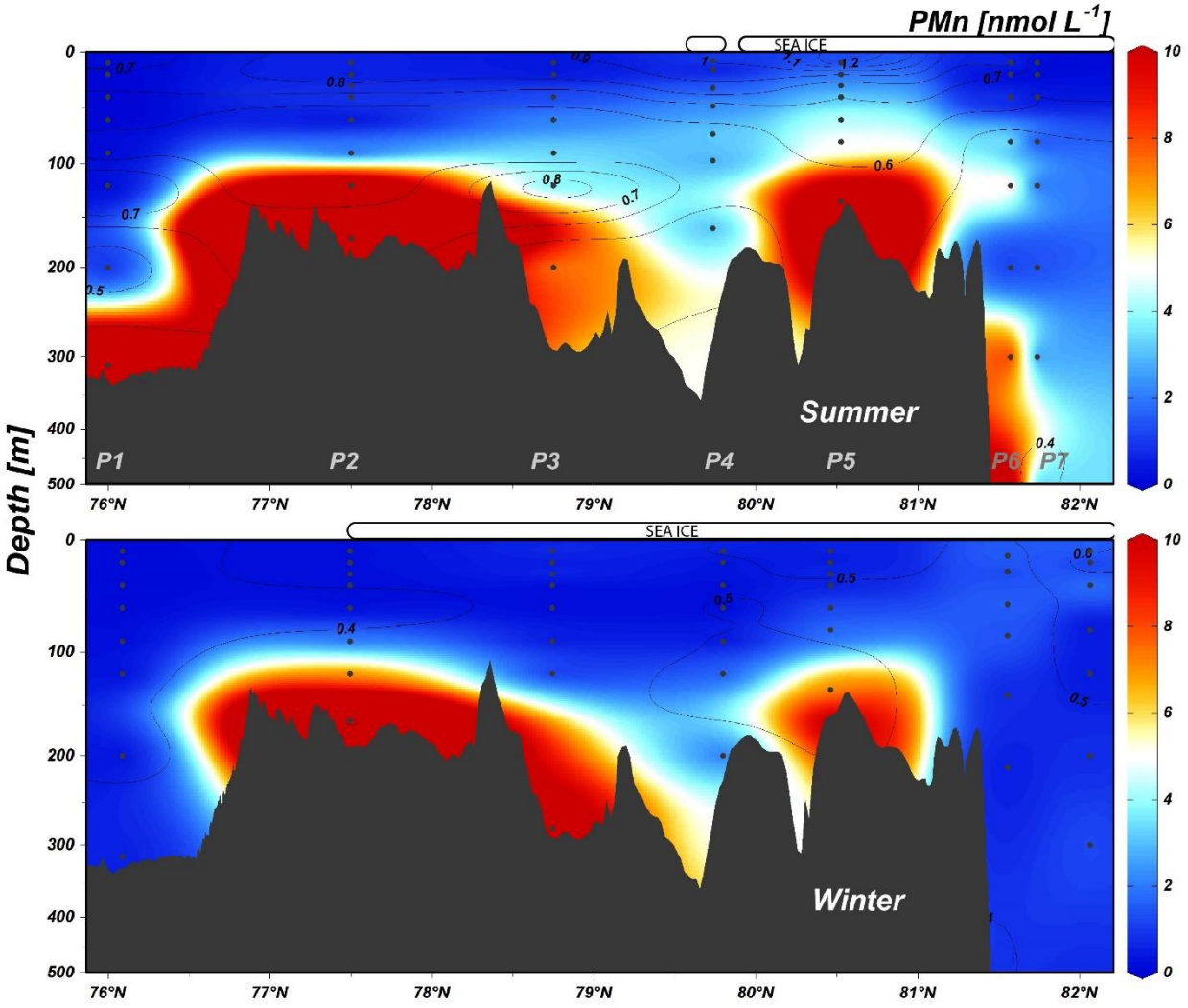

Extended Data Fig. 5. Particulate manganese (PMn) concentrations (nmol L^{-1}) along the shelf-deep basin gradient. Stations P1 – P7, (Latitude) are on the x-axis for summer 2019 (top) and winter 2019 cruises (bottom). Black contour lines for THg (pmol L^{-1}) from each corresponding season are overlain. Concentrations greater than the presented range (10 nmol L^{-1}) are plotted as the maximum.

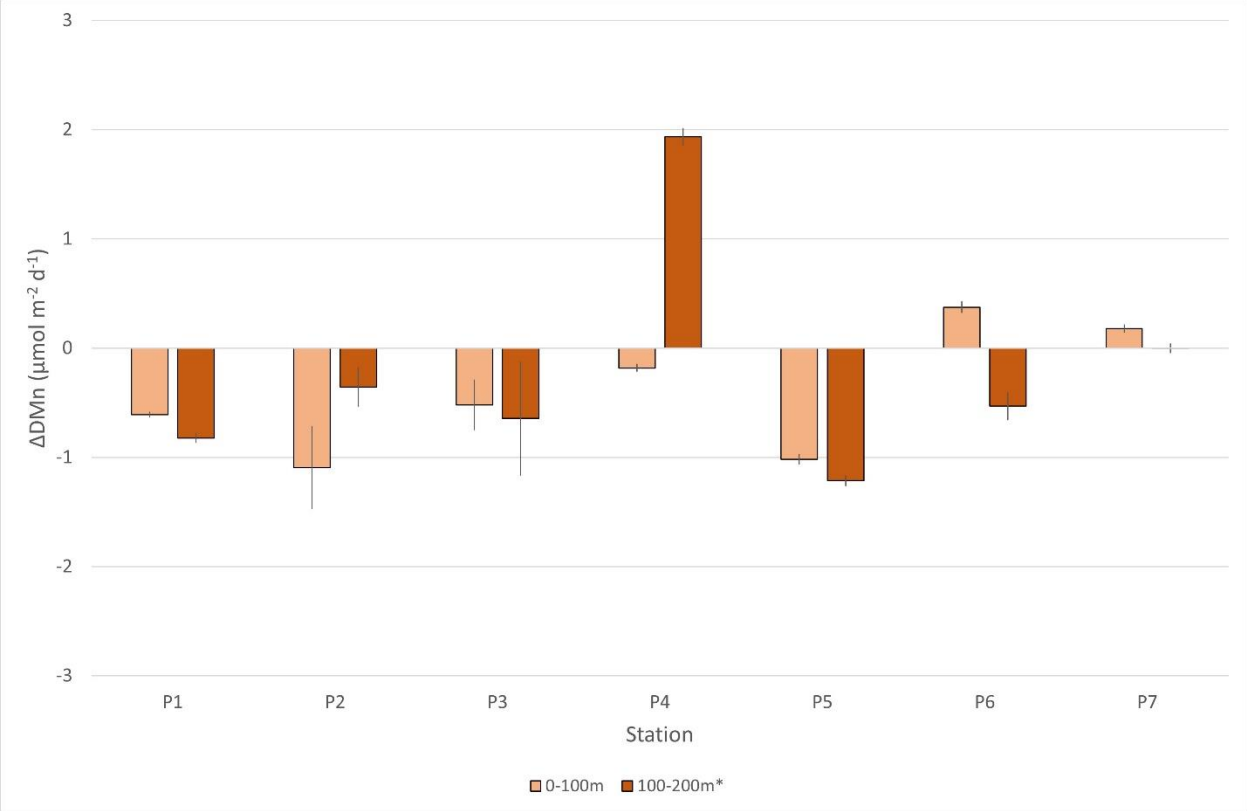

Extended Data Fig. 6. ΔDMn (µmol m^{-2} d^{-1}) at specified depth intervals for each station. A positive Δ value indicates a temporal gain in the DMn pool while a negative Δ value indicates a temporal loss in the DMn pool. Δ values are reported with error bars as combined standard uncertainty (±1σ). *Stations P2 and P5 were integrated from 100 m to sample depth less than 200 m.

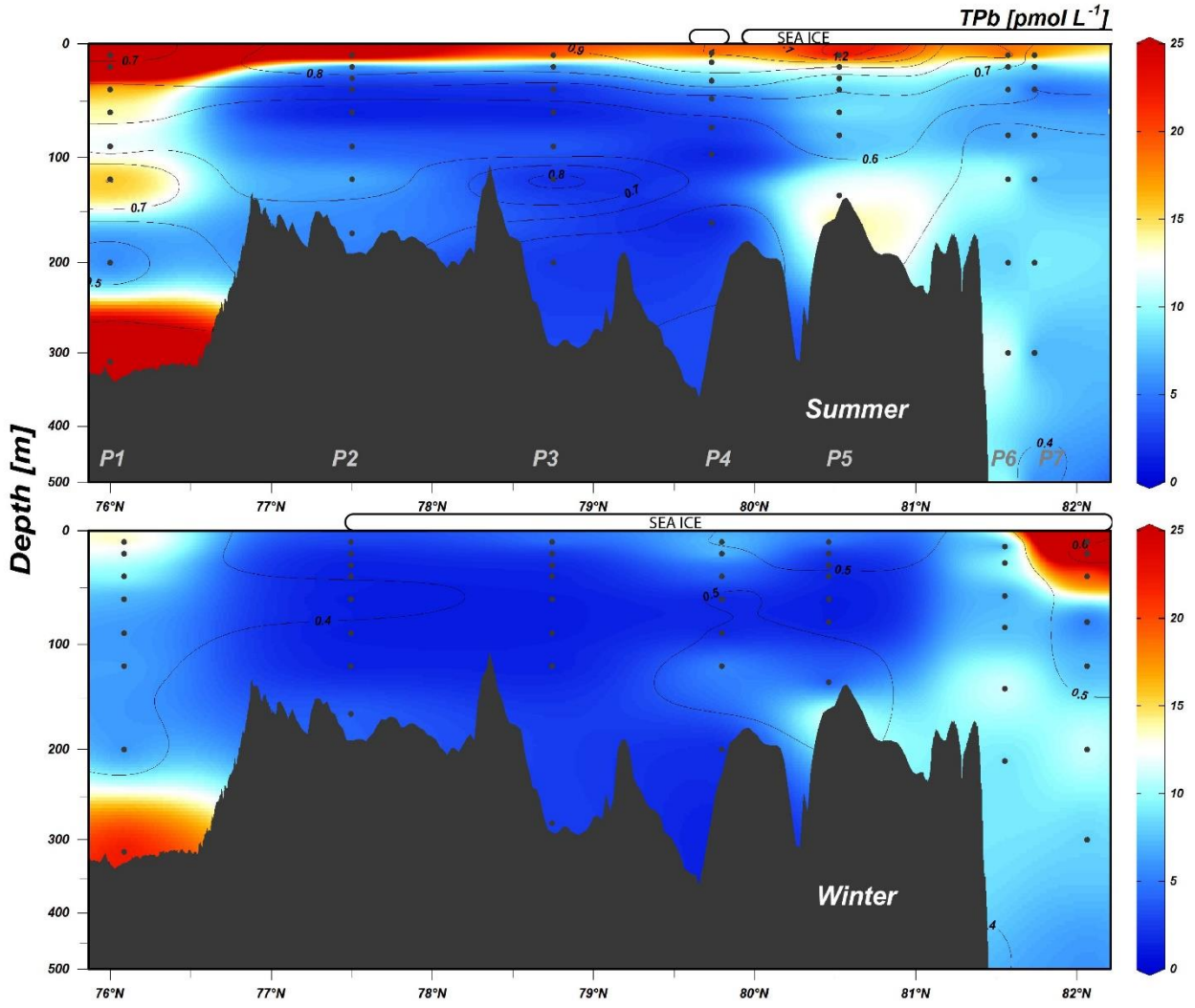

512

513 **Extended Data Fig. 7. Total acid-leachable lead (TPb) concentrations (pmol L^{-1}) along the**
514 **shelf-deep basin gradient**. Stations P1 – P7, (Latitude) are on the x-axis for summer 2019 (top)
515 and winter 2019 cruises (bottom). Data points at or below the detection limit were assigned the
516 value of the detection limit (1.08 pmol L^{-1}) determined by the seaFAST-pico ICP-MS for plotting
517 purposes. Black contour lines for THg (pmol L^{-1}) from each corresponding season are overlain.
518 Concentrations greater than the presented range (25 pmol L^{-1}) are plotted as the maximum.

519

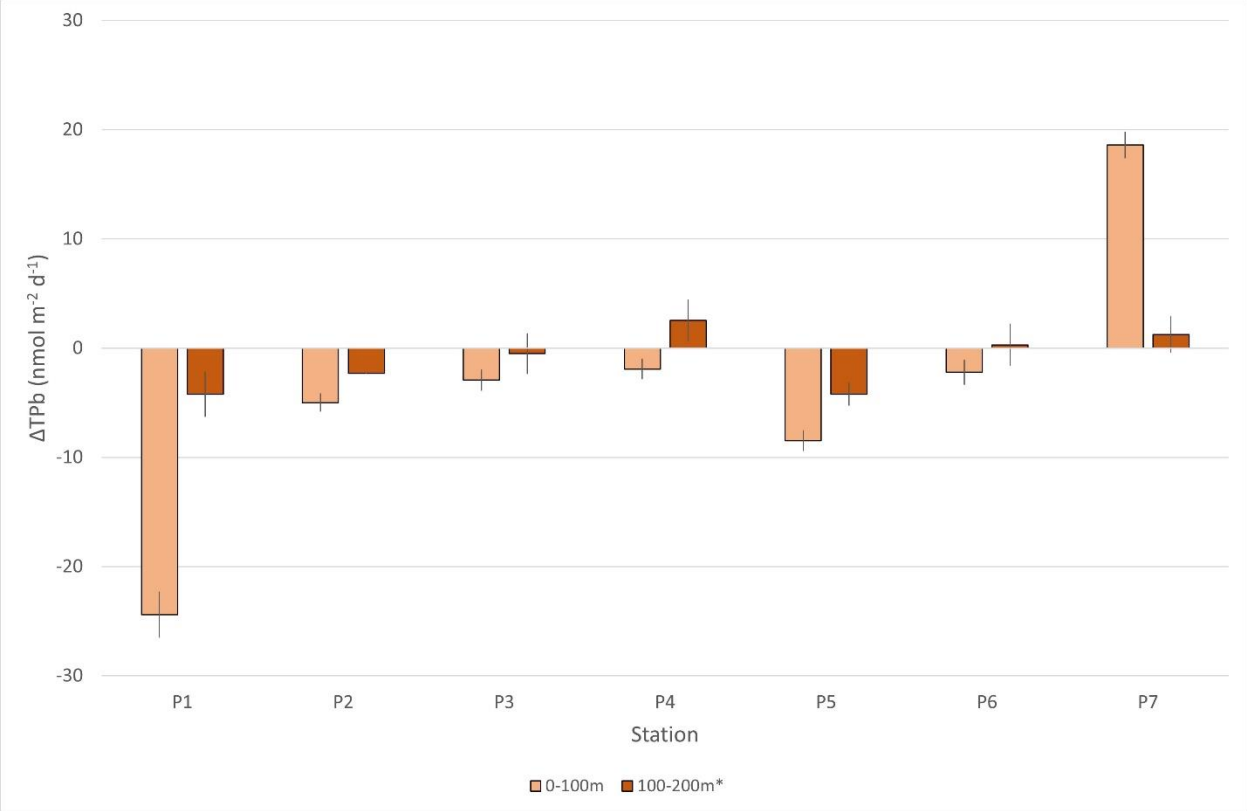

Extended Data Fig. 8. Extended Data Figure 8: ΔTPb (nmol m^{-2} d^{-1}) at specified depth interval for each station. A positive Δ value indicates a temporal gain in the TPb pool while a negative Δ value indicates a temporal loss in the TPb pool. Δ values are reported with error bars as combined standard uncertainty (±1σ). *Stations P2 and P5 were integrated from 100 m to sample depth less than 200 m.